mathematics

Article

Synchronization for Reaction–Diffusion Switched Delayed Feedback Epidemic Systems via Impulsive Control

Ruofeng Rao [1,2,*] and Quanxin Zhu [3,*]

[1] College of Mathematics, Chengdu Normal University, Chengdu 611130, China
[2] School of Mathematical and Computational Science, Hunan University of Science and Technology, Xiangtan 411201, China
[3] School of Mathematics and Statistics, Hunan Normal University, Changsha 410081, China
* Correspondence: ruofengrao@cdnu.edu.cn (R.R.); zqx22@hunnu.edu.cn (Q.Z.)

Abstract: Due to the facts that epidemic-related parameters vary significantly in different stages of infectious diseases and are relatively stable within the same stage, infectious disease models should be switch-type models. However, research on switch-type infectious disease models is scarce due to the complexity and intricate design of switching rules. This scarcity has motivated the writing of this paper. By assuming that switching instants and impulse times occur at different moments, this paper proposes switch rules suitable for impulse control and derives synchronization criteria for reaction–diffusion switch-type infectious disease systems under impulse control. The effectiveness of this method is validated through numerical simulations. It is important to mention that, based on the information available to us, this paper is currently the sole study focusing on switch-type reaction–diffusion models for infectious diseases.

Keywords: reaction–diffusion; Lyapunov–Krasovskii functional; switched epidemic systems; impulsive control

MSC: 34K24; 34K45

Citation: Rao, R.; Zhu, Q. Synchronization for Reaction–Diffusion Switched Delayed Feedback Epidemic Systems via Impulsive Control. *Mathematics* **2024**, *12*, 447. https://doi.org/10.3390/math12030447

Academic Editor: Giancarlo Consolo

Received: 28 December 2023
Revised: 24 January 2024
Accepted: 26 January 2024
Published: 30 January 2024

1. Introduction

As is well known, infectious diseases exhibit significant diffusion effects, and, thus, reaction–diffusion epidemic models have been recently studied in the literature. Stability analysis and synchronization control of infectious disease models have theoretical implications in practical epidemic management [1,2]. For instance, in reference [3], the author explored the stability of the wavefront in a delayed monostable reaction–diffusion epidemic system. The motivation behind the extensive focus on the dynamical stability of infectious disease models is rooted in the inherent difficulty of completely eliminating such diseases. Achieving stability in the interaction between susceptible and infected populations is a crucial objective in the realm of infectious disease prevention and control [3–10]. Reference [4], for example, conducted research on susceptible–infected–recovered dynamics, taking into account the impact of the healthcare system. Their study considered a general incidence rate function and recovery rate dependent on the number of hospital beds, establishing the existence, uniqueness, and boundedness of the model. It extensively investigated all possible steady-state solutions and their stability. In another case, reference [5] explored an epidemic model incorporating an incubation period, newborns, and vaccination for susceptible individuals. Their study demonstrated global stability through Lyapunov functions. Reference [6] derived stability conditions for an infectious disease model with delays by constructing appropriate Lyapunov functionals. Reference [7] delved into an SIR epidemic model with nonlinear incidence and delay, discussing the local stability of equilibrium states, both disease-free and endemic, through the analysis of the corresponding characteristic equation. Moreover, synchronization control of infectious disease models holds theoretical significance in practical epidemic management [1,2,11–15]. Reference [11] highlighted long-term spatiotemporal disease occurrence data indicating synchronization in many frequently occurring epidemics, especially childhood infections, between suburbs. The authors employed modeling techniques to elucidate the existence of synchronization phenomena. Reference [12] proposed a synchronization-based method for identifying parameters and estimating latent variables from real data in epidemic models. An adaptive synchronization method, based on an observer approach, was suggested, utilizing effective guiding parameters derived solely from real data. To validate identifiability and estimation results, a numerical simulation of a tuberculosis model was conducted using actual data from the central region of Cameroon. This study demonstrated that certain tools of nonlinear system synchronization can aid in addressing parameter and state estimation problems in the field of epidemiology. Reference [13] investigated synchronization between two identical susceptible–infected–recovered chaotic systems with fractional-order time derivatives.

The inclusion of a specific incubation period in infectious diseases necessitates the incorporation of models with delayed feedback in the mathematical modeling of these diseases. However, research in this field is very rare, which has motivated the writing of this article. Additionally, infectious diseases exhibit significant differences at different stages, and switch systems provide a good representation of infectious disease models. However, switch-type infectious disease models are seldom studied, providing another motivation for this article. Therefore, this article aims to investigate reaction–diffusion delayed feedback epidemic systems and intends to achieve synchronous control of infectious disease switch models through the use of pulse control techniques.

This article introduces innovations in three aspects:

◊ For the first time, this article introduces synchronous control of switch-type infectious disease models.
◊ For the first time, this article develops switching rules for infectious disease models.
◊ For the first time, this article successfully derives global exponential synchronization criteria specifically for impulse reaction–diffusion infectious disease models.

2. System Description

Recently, reaction–diffusion epidemic models have been studied in the literature. For instance, in the year 2020, reference [1] considered a reaction–diffusion epidemic model. In the year 2022, the authors of reference [2] investigated a delayed impulse reaction–diffusion epidemic model.

$$\begin{cases} \dfrac{\partial X(x,t)}{\partial t} = D\Delta X(x,t) + A(t)X(x,t) + \beta(t)f(t,X(x,t)), & x \in \Omega,\ t \geqslant t_0,\ t \neq t_k, \\ X(t_k^+,x) - X(t_k^-,x) = M_k X(t_k - v_k, x), & k \in \mathbb{N},\ x \in \Omega, \\ \dfrac{\partial X(x,t)}{\partial \nu} = 0, & x \in \partial\Omega,\ t \geqslant 0, \end{cases} \tag{1}$$

where $X(x,t) = (X_1(x,t), X_2(x,t), X_3(x,t))^T$, and the function $X_1(x,t)$ is the fraction of the susceptible population, $X_2(x,t)$ is the infected fraction, $X_3(x,t)$ is the recovered fraction, and $0 < X_i < 1$ for $i = 1,2,3$. In addition,

$$D = \begin{pmatrix} d_1 & 0 & 0 \\ 0 & d_2 & 0 \\ 0 & 0 & d_3 \end{pmatrix}, \quad A(t) = \begin{pmatrix} 0 & 0 & 0 \\ 0 & -\gamma(t) & 0 \\ 0 & \gamma(t) & 0 \end{pmatrix}, \quad f(t,X) = \begin{pmatrix} -X_1X_2 \\ X_1X_2 \\ 0 \end{pmatrix}, \tag{2}$$

Moreover, the disease transmission rate is denoted by $\beta(t)$, and the recovery rate is denoted by $\gamma(t)$. Taking into account the practical situation of delayed feedback in epidemic models, this paper considers the following delayed feedback epidemic model:

$$\begin{cases} \dfrac{\partial X(x,t)}{\partial t} = D_\sigma \Delta X(x,t) + A_\sigma X(x,t) + \beta_\sigma f(t, X(x,t)) + K_\sigma(X(x,t) - X(t-v(t),x)), & x \in \Omega,\ t \geqslant t_0,\ t \neq t_k, \\ X(t_k, x) = M_k X(t_k^-, x), & k \in \mathbb{N},\ x \in \Omega, \\ X(x,t) = 0, & x \in \partial\Omega,\ t \geqslant 0, \end{cases} \tag{3}$$

where K_σ is a family of positive definite diagonal matrices, which represents the delayed feedback parameters under the switching mode σ. Here, $\sigma \in \overline{N} \triangleq \{1, 2, \cdots, N\}$. t_k represents the moments of pulses, satisfying $0 < t_1 < t_2 < \cdots < t_k < t_{k+1} < \cdots$ with $\lim\limits_{k\to\infty} t_k = +\infty$. Assume that $X_i(t_k^+) = \lim\limits_{t \to t_k^+} X_i(t) = X_i(t_k)$, $i = 1, 2, 3$.

$$D_\sigma = \begin{pmatrix} d_{\sigma 1} & 0 & 0 \\ 0 & d_{\sigma 2} & 0 \\ 0 & 0 & d_{\sigma 3} \end{pmatrix}, \quad A_\sigma = \begin{pmatrix} 0 & 0 & 0 \\ 0 & -\gamma_\sigma & 0 \\ 0 & \gamma_\sigma & 0 \end{pmatrix}, \quad f(t, X) = \begin{pmatrix} -X_1 X_2 \\ X_1 X_2 \\ 0 \end{pmatrix}. \tag{4}$$

Here, β_σ and γ_σ are positive scalars for $\sigma \in \overline{N}$, and D_σ is the diffusion coefficient matrix.

System (3) is the drive system , and its response system can be considered as follows:

$$\begin{cases} \dfrac{\partial Y(x,t)}{\partial t} = D_\sigma \Delta Y(x,t) + A_\sigma Y(x,t) + \beta_\sigma f(t, Y(x,t)) + K_\sigma(Y(x,t) - Y(t-v(t),x)), & x \in \Omega,\ t \geqslant t_0,\ t \neq t_k, \\ Y(t_k, x) = M_k Y(t_k^-, x), & k \in \mathbb{N},\ x \in \Omega, \\ Y(x,t) = 0, & x \in \partial\Omega,\ t \geqslant 0, \end{cases} \tag{5}$$

Then, the error system is proposed as follows:

$$\begin{cases} \dfrac{\partial e(x,t)}{\partial t} = D_\sigma \Delta e(x,t) + A_\sigma e(x,t) + \beta_\sigma F(t, e(x,t)) + K_\sigma(e(x,t) - e(t-v(t),x)), & x \in \Omega,\ t \geqslant t_0,\ t \neq t_k, \\ e(t_k, x) = M_k e(t_k^-, x), & k \in \mathbb{N},\ x \in \Omega, \\ e(x,t) = 0, & t \geqslant 0,\ x \in \partial\Omega, \\ e(0,x) = \varphi(x), & x \in \Omega, \end{cases} \tag{6}$$

where $e = X - Y$, $v(t)$ is the time delay with $v(t) \in [-v, 0]$ and $v > 0$.

$$F(e(x,t)) = f(t, X(x,t)) - f(t, Y(x,t)) = \begin{pmatrix} -X_1X_2 + Y_1Y_2 \\ X_1X_2 - Y_1Y_2 \\ 0 \end{pmatrix} \tag{7}$$

Additionally, D_σ, A_σ, and f are defined in (4).

Obviously, $-1 < e_i < 1$.

Definition 1. *If the error system (6) is globally exponentially stable with a convergence rate of $\frac{\lambda}{2}$, then we say that system (5) globally exponentially synchronizes to system (3) with a synchronization rate of $\frac{\lambda}{2}$.*

Definition 2. *To establish the switching rule $\mathfrak{F}$:*

$$\sigma(t) = \arg\min \xi^T T_\sigma \xi. \tag{8}$$

($\mathfrak{F}_1$) Choose the initial mode $\sigma(t) = i_0$, if $\xi(t_0) \in \Gamma_{i_0}$.

($\mathfrak{F}_2$) For each $t > t_0$, if $\sigma(t^-) = i$ and $\xi \in \Gamma_i$, keep $\sigma(t) = i$. On the other hand, if $\sigma(t^-) = i$ but $\xi \notin \Gamma_i$, i.e., hitting a switching surface, choose the next mode by applying (8) and begin to switch.

Here, we assume that the switching moment and the impulse moment do not occur simultaneously and

$$\Gamma_i = \{\xi \in R^3,\ \xi^T T_i \xi < 0\},\ i = 1, 2, \cdots, N, \tag{9}$$

$$T_\sigma \triangleq \frac{\lambda_{\max}(\Theta_\sigma)}{\lambda_{\min}(P)} P - (\varsigma - \lambda)P,$$

and

$$\Theta_\sigma = -\lambda_1(PD_\sigma + D_\sigma P) + PA_\sigma + A_\sigma^T P + PK_\sigma + K_\sigma P + 5\beta_\sigma E + PK_\sigma + \mu e^{\lambda v}\lambda_{\max}(K_\sigma)P,$$

where $\mu \geqslant 1$ is a scalar, E is an identity matrix, P is an undetermined positive definite symmetric matrix, and λ_1 is the smallest positive eigenvalue of the following eigenvalue problem:

$$\begin{cases} -\Delta\varphi(x) = \lambda\varphi(x), & x \in \Omega \subset \mathbb{R}^n, \\ \varphi(x) = 0, & x \in \partial\Omega. \end{cases}$$

Remark 1. *Firstly, from Figure 1, we can see that the pulse moment and the switching moment do not occur simultaneously. That is, the state transition curve does not exhibit a pulse burst shape. The dynamic indications caused by the pulse only show significant changes around the switching points. Secondly, the idea of state-dependent switching can be briefly described in Figure 1. The solutions initiate from different initial points within mode 1 (Ω_1). Subsequently, upon reaching the boundary of mode 1, where it intersects exclusively with mode 2 (Ω_2), the system transitions to mode 2, as illustrated by the blue curve in Figure 1. Similarly, when reaching the boundary of mode 1 that intersects exclusively with mode 3 (Ω_3), the system switches to mode 3, represented by the red curve in Figure 1. Lastly, upon reaching the boundary of mode 1, which intersects with both mode 2 and mode 3, the system undergoes a switch to the mode determined by the minimum of law (8), as depicted by the black curve in Figure 1.*

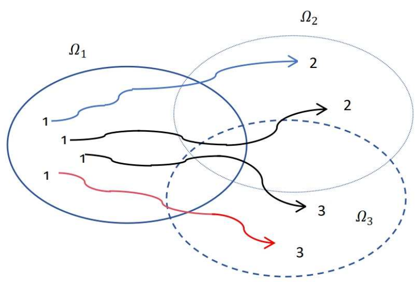

Figure 1. Switching behavior under impulse.

Lemma 1 ([16])**.** *Let $x \in R^n$, $y \in R^n$, and $\varepsilon > 0$. Then, we have*

$$x^T y + y^T x \leqslant \varepsilon x^T x + \varepsilon^{-1} y^T y.$$

Lemma 2 ([17])**.** *Suppose $V \in v_0$ and several positive scalars $p, c, k_1, k_2, \varsigma, \lambda > 0, \mu \geqslant 1$, and $\varsigma - \lambda \geqslant c$, satisfying:*

(i) $a_1\|x\|^p \leqslant V(t, x) \leqslant a_2\|x\|^p$, for any $t \in \mathbb{R}_+$ and $x \in \mathbb{R}^n$;

(ii) $\mathcal{D}^+V(t, \varphi(0)) \leqslant cV(t, \varphi(0))$, $t \in [t_{k-1}, t_k)$, $k \in \mathbb{N}$, whenever $qV(t, \varphi(0)) \geqslant V(t + s, \varphi(s))$ for $s \in [-v, 0]$, where $q \geqslant \mu e^{\lambda v}$ is a scalar;

(iii) $V(t_k, \varphi(0) + I_k(t_k, \varphi)) \leqslant d_k V(t_k^-, \varphi(0))$, where $0 < d_{k-1} \leqslant 1, \forall k \in \mathbb{N}$, are scalars;

(iv) $\varsigma \geqslant \frac{1}{d_{k-1}}$ and $\ln d_{k-1} < -(\varsigma + \lambda)(t_k - t_{k-1}), k \in \mathbb{N}$.

Then, the null solution of the delayed differential equation with impulse

$$\begin{cases} \dot{x}(t) = f(t, x_t), & t \neq t_k,\ t \geqslant t_0,\ k \in \mathbb{Z}_+; \\ \Delta x(t_k) = I_k(t_k, x_{t_k^-}) k \in \mathbb{Z}_+; \\ x_{t_0} = \varphi. \end{cases}$$

is globally exponentially stable with a convergent rate $\frac{\lambda}{p}$ *for any time delays* $v \in (0, \infty)$.

3. Main Results

Theorem 1. *System (5) globally exponentially asymptotically synchronizes with system (3), and its synchronization rate is* $\frac{\lambda}{2}$, *if the following conditions (a)–(c) are satisfied:*

(a) There is a scalar $m_0 > 0$ *such that*

$$0 < \lambda_{\max}(M_k) \leqslant m_0 < 1, \quad \forall k = 1, 2, \cdots \tag{10}$$

(b) There exist scalars $\varsigma > 0$ *and* $\lambda > 0$ *such that*

$$\varsigma \geqslant \frac{1}{m_0^2} \tag{11}$$

and

$$\ln m_0^2 < -(\varsigma + \lambda)(t_k - t_{k-1}), k \in \mathbb{N} \tag{12}$$

(c) There exist scalars $\alpha_i \geqslant 0$ *with* $\sum_{i=1}^{N} \alpha_i = 1$ *such that*

$$\Lambda \triangleq \sum_{i=1}^{N} \alpha_i \frac{\lambda_{\max}(\Theta_i)}{\lambda_{\min}(P)} P - (\varsigma - \lambda)P < 0. \tag{13}$$

Proof. Consider the following Lyapunov–Krasovskii functional,

$$V(t) = \int_\Omega e^T(x,t) P e(x,t) dx. \tag{14}$$

Let $\|e(t)\|^2 = \int_\Omega e^T(x,t) e(x,t) dx$, where P is a positive definite symmetric matrix. Then, there are $k_1, k_2 > 0$ such that

$$k_1 \|e(t)\|^2 \leqslant V(t) \leqslant k_2 \|e(t)\|^2,$$

which satisfies condition (i) of Lemma 2.

Due to $0 < X_i < 1, 0 < Y_i < 1$, and (7), we can see this by using the differential along the trajectory of system (6) that

$$\begin{aligned}
\mathcal{D}^+ V &= 2 \int_\Omega e^T(x,t) P \Big(D_\sigma \Delta e(x,t) + A_\sigma e(x,t) + \beta_\sigma F(t, e(x,t)) + K_\sigma (e(x,t) - e(t - v(t), x)) \Big) dx \\
&\leqslant \int_\Omega e^T(x,t) \Big(-\lambda_1 (P D_\sigma + D_\sigma P) + P A_\sigma + A_\sigma^T P + P K_\sigma + K_\sigma P \Big) e(x,t) dx + 2\beta_\sigma \int_\Omega e^T(t) F(t, e(t)) dx \\
&\quad - 2 \int_\Omega e^T(t) P K_\sigma e(t - v(t)) dx \\
&\leqslant \int_\Omega e^T(x,t) \Big(-\lambda_1 (P D_\sigma + D_\sigma P) + P A_\sigma + A_\sigma^T P + P K_\sigma + K_\sigma P + 5\beta_\sigma E + P K_\sigma \Big) e(x,t) dx \\
&\quad + \int_\Omega e^T(t - v(t)) P K_\sigma e(t - v(t)) dx \\
&\leqslant \int_\Omega e^T(x,t) \Big(-\lambda_1 (P D_\sigma + D_\sigma P) + P A_\sigma + A_\sigma^T P + P K_\sigma + K_\sigma P + 5\beta_\sigma E + P K_\sigma \Big) e(x,t) dx \\
&\quad + \int_\Omega e^T(t - v(t)) P K_\sigma e(t - v(t)) dx
\end{aligned} \tag{15}$$

If there exists $\mu \geqslant 1$ such that $\mu e^{\lambda v} \int_\Omega e^T(x,t) P e(x,t) dx \geqslant \int_\Omega e^T(t - v(t), x) P e(t - v(t), x) dx$, by (15), we can obtain that

$$\mathcal{D}^+V \leqslant \int_\Omega e^T(x,t)\Big(-\lambda_1(PD_\sigma + D_\sigma P) + PA_\sigma + A_\sigma^T P + PK_\sigma + K_\sigma P + 5\beta_\sigma E + PK_\sigma + \mu e^{\lambda v}\lambda_{\max}(K_\sigma)P\Big)e(x,t)dx$$
$$\leqslant \int_\Omega e^T(x,t)\lambda_{\max}(\Theta_\sigma)e(x,t)dx \leqslant \frac{\lambda_{\max}(\Theta_\sigma)}{\lambda_{\min}(P)}\int_\Omega e^T(x,t)Pe(x,t)dx = \frac{\lambda_{\max}(\Theta_\sigma)}{\lambda_{\min}(P)}V(t) \quad (16)$$

Next, we will derive the following inequlity based on the switching rule $\mathfrak{F}$ from (16).

$$\mathcal{D}^+V \leqslant (\varsigma - \lambda)\int_\Omega e^T(x,t)Pe(x,t)dx. \quad (17)$$

Firstly, we claim that

$$\bigcup_{i=1}^N \Gamma_i = R^3 \setminus \{0\} \quad (18)$$

Indeed, since there exist scalars $\alpha_i \geqslant 0$ with $\sum\limits_{i=1}^N \alpha_i = 1$ such that $\Lambda \triangleq \sum\limits_{i=1}^N \alpha_i \frac{\lambda_{\max}(\Theta_i)}{\lambda_{\min}(P)}P - (\varsigma - \lambda)P < 0$. Hence, utilizing proof by contradiction, it is not difficult to deduce the validity of equation (18). With the establishment of equation (18), we can now prove the validity of (17).

In fact, according to the switching law $\mathfrak{F}$, when $\sigma(t^-) = i$ and $e(x,t) \in \Gamma_i$, we can obtain, by the definition of T_i, that

$$0 > e(x,t)^T T_i e(x,t) = e(x,t)^T[\frac{\lambda_{\max}(\Theta_i)}{\lambda_{\min}(P)} - (\varsigma - \lambda)]e(x,t)^T$$

$$\mathcal{D}^+V \leqslant \frac{\lambda_{\max}(\Theta_i)}{\lambda_{\min}(P)}\int_\Omega e^T(x,t)Pe(x,t)dx \leqslant (\varsigma - \lambda)\int_\Omega e^T(x,t)Pe(x,t)dx$$

Note that the above expression also holds when $e(x,t) = 0$. Therefore, overall, we only need to consider the case where $e(x,t) \neq 0$.

When $\sigma(t^-) = i$ and $e(x,t) \notin \Gamma_i$, this means that the trajectory hits a switching surface. Due to (18), the minimum law (8) deduces that there must exist a Γ_j such that $e(x,t) \in \Gamma_j$ and

$$0 > e(x,t)^T T_j e(x,t) = e(x,t)^T[\frac{\lambda_{\max}(\Theta_j)}{\lambda_{\min}(P)} - (\varsigma - \lambda)]e(x,t)^T$$

$$\mathcal{D}^+V \leqslant \frac{\lambda_{\max}(\Theta_j)}{\lambda_{\min}(P)}\int_\Omega e^T(x,t)Pe(x,t)dx \leqslant (\varsigma - \lambda)\int_\Omega e^T(x,t)Pe(x,t)dx$$

To this end, we obtain $\mathcal{D}^+V \leqslant (\varsigma - \lambda)\int_\Omega e^T(x,t)Pe(x,t)dx$ if $\mu e^{\lambda v}V(t) \geqslant V(t - v(t))$, i.e.,

$$\mu e^{\lambda v}\int_\Omega e^T(x,t)Pe(x,t)dx \geqslant \int_\Omega e^T(t - v(t),x)Pe(t - v(t),x)dx$$

In other words, condition (ii) of Lemma 2 is satisfied.

Additionally,

$$V(t_k) = \int_\Omega e^T(t_k,x)Pe(t_k,x)dx = \int_\Omega e^T(t_k^-,x)M_k^T P M_k e(t_k^-,x)dx \leqslant m_0^2 V(t_k^-),$$

which implies that condition (iii) of Lemma 2 holds.

Furthermore, based on the conditions of Theorem 1, condition (iv) of Lemma 2 is satisfied.

Therefore, according to Lemma 2, error system (6) is globally exponentially stable with a convergence rate of $\frac{\lambda}{2}$. In other words, system (5) is globally exponentially synchronized with system (3), and its synchronization rate is $\frac{\lambda}{2}$. $\square$

Remark 2. *Theorem 1 ingeniously addresses the challenges of synchronizing control that arise from the interplay of reaction–diffusion processes, time delays, and impulsive control. Specifically, it overcomes the mathematical difficulties induced by the diffusion term by employing Poincare inequalities, designs an appropriate Lyapunov function, sets suitable pulse intervals and pulse intensities, and, ultimately, achieves synchronization control through the utilization of the delayed-impulse inequalities lemma.*

Remark 3. *The switching rule of Theorem 1 is different from the switching rule in reference [18]. Meanwhile, synchronization control results for epidemic models have been achieved using impulse control. This is the first time that synchronization control has been obtained for a reaction–diffusion epidemic model under a switching rule.*

Discussion 1. *In epidemic prevention and control, the impulse moment is artificially determined and may not coincide with the switching moment. Therefore, this paper assumes that the impulse moment and switching moment do not occur simultaneously, which is reasonable. However, if one were to consider their simultaneous occurrence, the design of switching rules in this paper would need further consideration and discussion. This poses an interesting question worth exploring in more depth.*

Discussion 2. *Stochastic perturbations and stochastic models are widely employed in various fields, including infectious disease models ([6,19,20]). Exploring how to control the dynamics of infectious diseases through impulse control under stochastic perturbations is an intriguing question.*

4. Numerical Example

Now, we verify the effectiveness of Theorem 1 via the following numerical example.

Example 1. *Let* $\Omega = [0,1] \times [0,1] \subset R^2$*. Then,* $\lambda_1 = 2\pi^2 = 19.7392$ *([21], Remark 14). In addition, set* $N = 3$ *and* $\overline{N} = \{1,2,3\}$*. Then,* $\sigma \in \{1,2,3\}$*. Let* $\beta_1 = 0.1$*,* $\beta_2 = 0.15$*,* $\beta_3 = 0.2$*, and*

$$D_1 = \begin{pmatrix} 0.4 & 0 & 0 \\ 0 & 0.3 & 0 \\ 0 & 0 & 0.3 \end{pmatrix}, \quad A_1 = \begin{pmatrix} 0 & 0 & 0 \\ 0 & -0.1 & 0 \\ 0 & 0.1 & 0 \end{pmatrix}, \quad K_1 = \begin{pmatrix} 0.15 & 0 & 0 \\ 0 & 0.13 & 0 \\ 0 & 0 & 0.13 \end{pmatrix},$$

$$D_2 = \begin{pmatrix} 0.35 & 0 & 0 \\ 0 & 0.37 & 0 \\ 0 & 0 & 0.4 \end{pmatrix}, \quad A_2 = \begin{pmatrix} 0 & 0 & 0 \\ 0 & -0.15 & 0 \\ 0 & 0.15 & 0 \end{pmatrix}, \quad K_2 = \begin{pmatrix} 0.2 & 0 & 0 \\ 0 & 0.15 & 0 \\ 0 & 0 & 0.18 \end{pmatrix},$$

$$D_3 = \begin{pmatrix} 0.5 & 0 & 0 \\ 0 & 0.4 & 0 \\ 0 & 0 & 0.38 \end{pmatrix}, \quad A_3 = \begin{pmatrix} 0 & 0 & 0 \\ 0 & -0.2 & 0 \\ 0 & 0.2 & 0 \end{pmatrix}, \quad K_3 = \begin{pmatrix} 0.19 & 0 & 0 \\ 0 & 0.23 & 0 \\ 0 & 0 & 0.23 \end{pmatrix}.$$

Set $P = E$*,* $\mu = 1, v = 1,$ *and* $\lambda = 1$*. Then,*

$$\Theta_1 = \begin{pmatrix} -14.4336 & 0 & 0 \\ 0 & -10.7458 & 0.1000 \\ 0 & 0.1000 & -10.5458 \end{pmatrix}, \quad \Theta_2 = \begin{pmatrix} -11.9238 & 0 & 0 \\ 0 & -13.1634 & 0.1500 \\ 0 & 0.1500 & -13.9577 \end{pmatrix},$$

$$\Theta_3 = \begin{pmatrix} -17.5340 & 0 & 0 \\ 0 & -13.9562 & 0.2000 \\ 0 & 0.2000 & -12.7366 \end{pmatrix}$$

$$\lambda_{\max}(\Theta_1) = -10.5044, \quad \lambda_{\max}(\Theta_2) = -11.9238, \quad \lambda_{\max}(\Theta_3) = -12.7046$$

$$\Theta_\sigma = -\lambda_1(PD_\sigma + D_\sigma P) + PA_\sigma + A_\sigma^T P + PK_\sigma + K_\sigma P + 5\beta_\sigma E + PK_\sigma + \mu e^{\lambda v}\lambda_{\max}(K_\sigma)P,$$

$$T_\sigma \triangleq \frac{\lambda_{\max}(\Theta_\sigma)}{\lambda_{\min}(P)}P - (\varsigma - \lambda)P,$$

Let

$$M_k = \begin{pmatrix} 0.9 & 0 & 0 \\ 0 & 0.89 & 0 \\ 0 & 0 & 0.88 \end{pmatrix}, k = 1, 2, \cdots$$

Then

$$m_0 = 0.9, \;\; m_0^2 = 0.81, \;\; \frac{1}{m_0^2} = 1.2346, \;\; \ln m_0^2 = -0.2107$$

Let $\varsigma = 1.3 > \frac{1}{m_0^2}$, $t_k - t_{k-1} \equiv 0.09$. *Then we obtain*

$$0 < \lambda_{\max}(M_k) \leqslant m_0 = 0.9 < 1, \quad \forall k = 1, 2, \cdots$$

$$\varsigma = 1.3 > \frac{1}{m_0^2}$$

and

$$\ln m_0^2 = -0.2107 < -0.2070 = -(\varsigma + \lambda)(t_k - t_{k-1}), \, k \in \mathbb{N}$$

Finally, let $\alpha_i = \frac{1}{3} \geqslant 0$ *with* $\sum_{i=1}^{3} \alpha_i = 1$. *We can see it that*

$$\Lambda = \sum_{i=1}^{3} \alpha_i \frac{\lambda_{\max}(\Theta_i)}{\lambda_{\min}(P)}P - (\varsigma - \lambda)P < 0.$$

Thus far, all conditions of Theorem 1 have been satisfied. Therefore, according to Theorem 1, error system (6) is globally exponentially stable with a convergence rate of $\frac{1}{2}$. *In other words, system (5) is globally exponentially asymptotically synchronized with system (3), and its synchronization rate is* $\frac{1}{2}$ *(see Figures 2–4).*

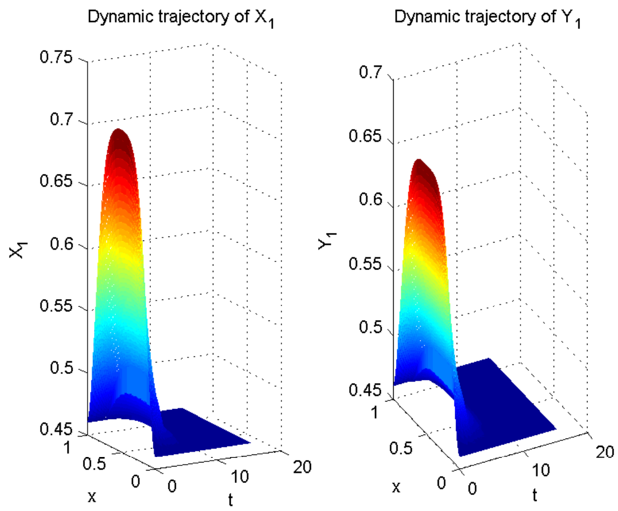

Figure 2. Numerical result of X_1 in (3) and Y_1 in (5).

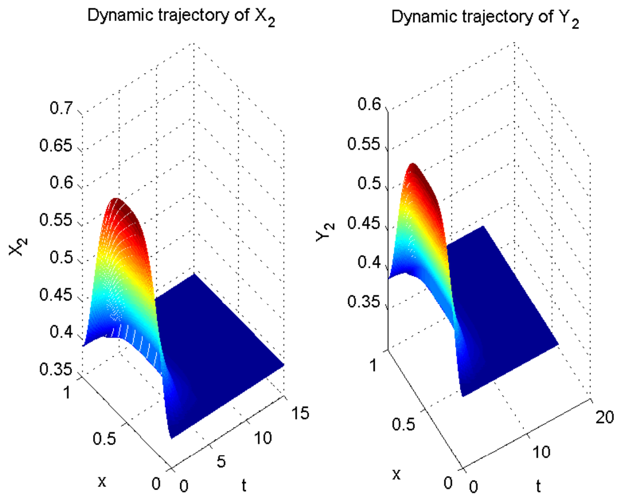

Figure 3. Numerical result of X_2 in (3) and Y_2 in (5).

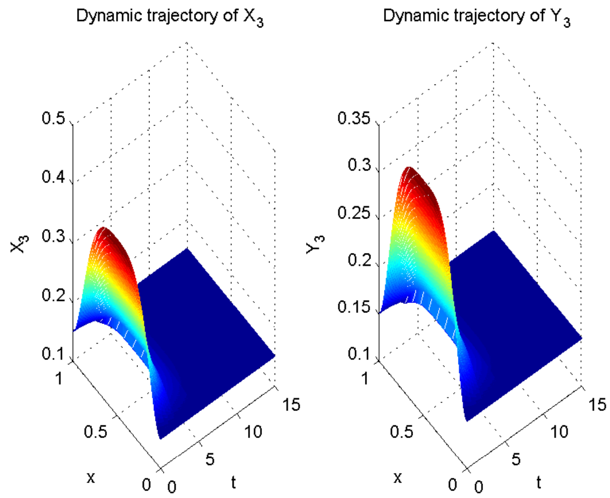

Figure 4. Numerical result of X_3 in (3) and Y_3 in (5).

Remark 4. *Numerical simulation results indicate that, despite the relatively small impulse strength, significant effectiveness in synchronizing control of the epidemic model can be achieved as long as an appropriate pulse interval is set. This validates the effectiveness of Theorem 1.*

Example 2. *In Example 1, let*

$$M_k = \begin{pmatrix} 0.5 & 0 & 0 \\ 0 & 0.5 & 0 \\ 0 & 0 & 0.49 \end{pmatrix}, \ k = 1, 2, \cdots$$

Then

$$m_0 = 0.5, \ \ m_0^2 = 0.25, \ \ \frac{1}{m_0^2} = 4, \ \ \ln m_0^2 = -1.3863$$

Let $\varsigma = 5$, $t_k - t_{k-1} \equiv 0.2$, *and other data of Example 1 hold unchanged. Then, we obtain* $\lambda = 1$ *and*

$$0 < \lambda_{\max}(M_k) \leqslant m_0 = 0.5 < 1, \quad \forall k = 1, 2, \cdots$$

$$\varsigma = 5 > 4 = \frac{1}{m_0^2}$$

and

$$\ln m_0^2 = -1.38637 < -1.2 = -(\varsigma + \lambda)(t_k - t_{k-1}),\ k \in \mathbb{N}$$

Finally, let $\alpha_i = \frac{1}{3} \geqslant 0$ *with* $\sum_{i=1}^{3} \alpha_i = 1$. *We can see it that*

$$\Lambda = \sum_{i=1}^{3} \alpha_i \frac{\lambda_{\max}(\Theta_i)}{\lambda_{\min}(P)} P - (\varsigma - \lambda)P < 0.$$

Thus far, all conditions of Theorem 1 have been satisfied. Therefore, according to Theorem 1, error system (6) is globally exponentially stable with a convergence rate of $\frac{1}{2}$. *In other words, system (5) is globally exponentially asymptotically synchronized with system (3), and its synchronization rate is* $\frac{1}{2}$ *(see Figures 5–7).*

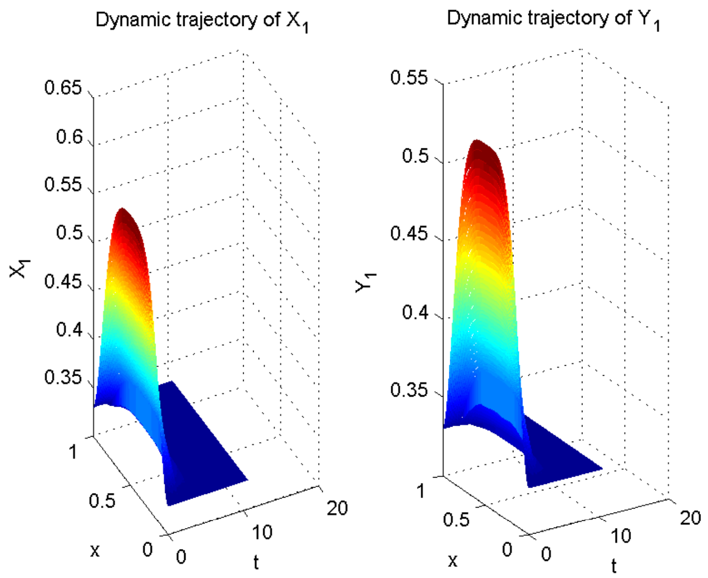

Figure 5. Numerical result of X_1 in (3) and Y_1 in (5).

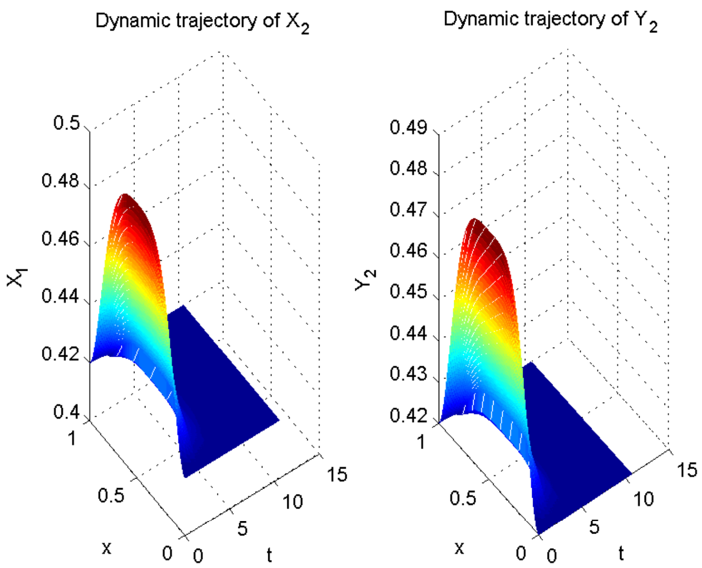

Figure 6. Numerical result of X_2 in (3) and Y_2 in (5).

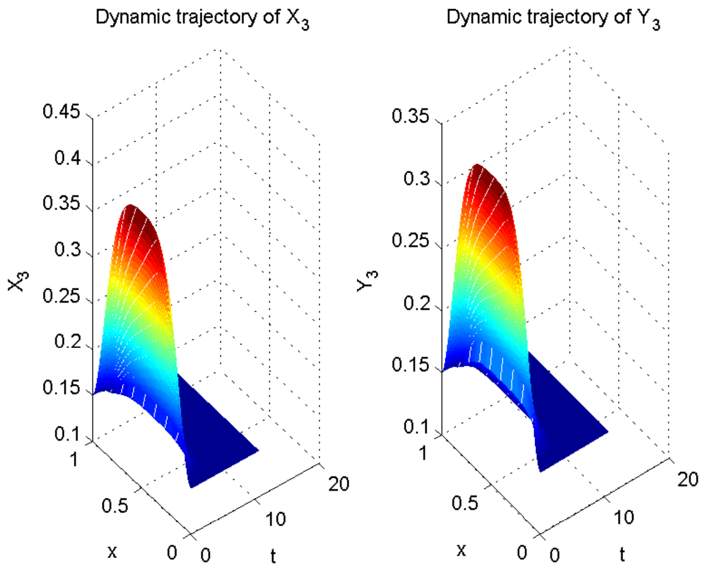

Figure 7. Numerical result of X_3 in (3) and Y_3 in (5).

Remark 5. *The numerical results indicate that, despite the enlargement of the impulse interval, as the impulse intensity increases, the convergence speed of synchronization still remains, which can be listed as Table 1:*

Table 1. Comparisons of Example 1 and Example 2.

	Impulse Interval	Impulse Frequency	Impulse Intensity	Intensity Degree	Convergent Rate
Example 1	0.09	↑	0.9	↓	1/2
Example 2	0.2	↓	0.5	↑	1/2

5. Conclusions

Synchronized control flow epidemic models have significant theoretical guidance, especially when there are substantial differences in the development stages of the epidemic. For instance, in the recent COVID-19 pandemic, various parameters, such as the number of infections and susceptible individuals, differ significantly across stages. The truth is that parameters related to different stages have notable distinctions. Impulse control, in essence, involves the momentary input intensity of artificial prevention measures and drug deployment treatment in different stages. Synchronized control under impulse measures allows for the gradual synchronization of heavily affected areas, where artificial measures are input in batches, in response to the evolving and fluctuating nature of the epidemic. This helps reduce the severity of the epidemic in heavily affected areas and gradually synchronize them with regions where the situation is improving. The synchronized control epidemic model offers significant theoretical guidance, especially when there are substantial differences in the development stages of the epidemic. Therefore, this paper considers a switching-type epidemic model. By establishing appropriate switching rules and utilizing impulse control techniques, global exponential synchronization criteria are obtained. Numerical examples demonstrate the effectiveness of the proposed methods. It is worth noting that this paper improves upon some existing methods in the literature and applies them for the first time to epidemic models, providing insights for a future series of related improvements.

Author Contributions: Conceptualization, R.R. and Q.Z.; methodology, R.R.; software, R.R.; validation, R.R. and Q.Z.; formal analysis, R.R. and Q.Z.; investigation, R.R.; resources, R.R.; data curation, R.R.; writing—original draft preparation, R.R.; writing—review and editing, R.R.; visualization, R.R.;

supervision, Q.Z.; project administration, Q.Z.; funding acquisition, Q.Z. All authors have read and agreed to the published version of the manuscript.

Funding: This research was funded by the Applied Basic Research Project of the Sichuan Provincial Department of Science and Technology (2020YJ0434).

Institutional Review Board Statement: Not applicable.

Informed Consent Statement: Not applicable.

Data Availability Statement: Data sharing is not applicable to this article.

Conflicts of Interest: The authors declare no conflict of interest.

References

1. Zhang, L.; Wang, Z.; Zhao, X. Time periodic traveling wave solutions for a Kermack-McKendrick epidemic model with diffusion and seasonality. *J. Evol. Equ.* **2020**, *20*, 1029–1059. [CrossRef]
2. Rao, R.; Lin, Z.; Ai, X.; Wu, J. Synchronization of Epidemic Systems with Neumann Boundary Value under Delayed Impulse. *Mathematics* **2022**, *10*, 2064. [CrossRef]
3. Yang, Y.; Li, W.; Wu, S. Exponential stability of traveling fronts in a diffusion epidemic system with delay. *Nonlinear Anal. RWA* **2011**, *12*, 1223–1234. [CrossRef]
4. Alqahtani, R. T. Mathematical model of SIR epidemic system (COVID-19) with fractional derivative: stability and numerical analysis. *Adv. Diff. Equ.* **2021**, *1*, 2. [CrossRef] [PubMed]
5. Li, J.; Yang, Y.; Zhou, Y. Global stability of an epidemic model with latent stage and vaccination. *Nonlinear Anal. RWA* **2011**, *12*, 2163–2173. [CrossRef]
6. Beretta, E.; Kolmanovskii, V.; Shaikhet, L. Stability of epidemic model with time delays influenced by stochastic perturbations. *Math. Comp. Simul.* **1998**, *45*, 269–277. [CrossRef]
7. Xu, R.; Ma, Z. Global stability of a SIR epidemic model with nonlinear incidence rate and time delay. *Nonlinear Anal. RWA* **2009**, *10*, 3175–3189. [CrossRef]
8. Khanafer, A.; Basar, T.; Gharesifard, B. Stability of epidemic models over directed graphs: A positive systems approach. *Automatica* **2016**, *74*, 126–134. [CrossRef]
9. Yi, N.; Zhang, Q.; Mao, K.; Yang, D.; Li, Q. Analysis and control of an SEIR epidemic system with nonlinear transmission rate. *Math. Comput. Model.* **2009**, *50*, 1498–1513. [CrossRef] [PubMed]
10. Zaman, G.; Kang, Y. H.; Jung, I. H. Stability analysis and optimal vaccination of an SIR epidemic model. *BioSystems* **2008**, *93*, 240–249. [CrossRef]
11. He, D.; Stone, L. Spatio-temporal synchronization of recurrent epidemics. *Proc. Royal Soc. Lond. Ser. B Biol. Sci.* **2003**, *270*, 1519–1526. [CrossRef] [PubMed]
12. Bowong, S., Kurths, J. Parameter estimation based synchronization for an epidemic model with application to tuberculosis in Cameroon. *Phys. Lett. A* **2010**, *374*, 4496–4505. [CrossRef]
13. Ansari, S. P.; Agrawal, S. K.; Das, S. Stability analysis of fractional-order generalized chaotic susceptible-infected-recovered epidemic model and its synchronization using active control method. *Pramana* **2015**, *84*, 23–32. [CrossRef]
14. Yan, G.; Fu, Z. Q.; Ren, J.; Wang, W. X. Collective synchronization induced by epidemic dynamics on complex networks with communities. *Phys. Rev. E* **2007**, *75*, 016108. [CrossRef]
15. Verma, T.; Gupta, A. K. Network synchronization, stability and rhythmic processes in a diffusive mean-field coupled SEIR model. *Commun. Nonlinear Sci. Numer. Simul.* **2021**, *102*, 105927 [CrossRef]
16. Wang, Z.; Liu, Y.; Yu, L.; Liu, X. Exponential stability of delayed recurrent neural networks with Markovian jumping parameters. *Phys. Lett. A* **2006**, *356*, 346–352. [CrossRef]
17. Wu, Q.; Zhou, J.; Xiang, L. Global exponential stability of impulsive differential equations with any time delays. *Appl. Math. Lett.* **2010**, *23*, 143–147. [CrossRef]
18. Yang, D.; Li, X.; Song, S. Design of state-dependent switching laws for stability of switched stochastic neural networks with time-delays. *IEEE Trans. Neural Netw. Learn. Syst.* **2020**, *31*, 1808–1819. [CrossRef]
19. Kumar, A. Light propagation through biological tissue: comparison between Monte Carlo simulation and deterministic models. *Int. J. Biomed. Eng. Technol.* **2009**, *2*, 344–351. [CrossRef]
20. Maini, D. S.; Aggarwal, A. K. Camera position estimation using 2D image dataset. *Int. J. Innov. Eng. Technol.* **2018**, *10*, 199–203.
21. Rao, R.; Huang, J.; Li, X. Stability analysis of nontrivial stationary solution and constant equilibrium point of reaction–diffusion neural networks with time delays under Dirichlet zero boundary value. *Neurocomputing* **2021**, *445*, 105–120. [CrossRef]